Electrochemical Characteristics of the Nanocrystalline and Amorphous $(Mg_{24}Ni_{10}Cu_2)_{100-x}Nd_x$ (x = 0–20) Alloys

Yanghuan Zhang, Tai Yang, Zeming Yuan, Wengang Bu, Zhonghui Hou, Ying Cai
Key Laboratory of Integrated Exploitation of Baiyun Obo Multi-Metal Resources
Inner Mongolia University of Science and Technology
Baotou, China
e-mail: zhangyh59@sina.com (Y. H. Zhang)

Dongliang Zhao
Department of Functional Material Research
Central Iron and Steel Research Institute
Beijing, China
e-mail: dlzhao@sina.com (D. L. Zhao)

***Abstract*—The $(Mg_{24}Ni_{10}Cu_2)_{100-x}Nd_x$ (x = 0–20) alloys are fabricated by vacuum induction melting and melt-spinning technique. The structures of the as-cast and spun alloys were characterized by X-ray diffraction (XRD) and transmission electron microscopy (TEM). The electrochemical hydrogen storage performances of the alloys were also tested by an automatic galvanostatic system. It was found that all the as-cast alloys hold a multiphase structure, containing Mg_2Ni-type major phase and the secondary phase $NdMg_{12}$. Furthermore, it must be noted that the amorphization degree of the alloys visibly increases with the rising of Nd content, suggesting that the addition of Nd facilitates the glass forming in the Mg_2Ni-type alloy. The maximum discharge capacities and the capacity retaining rate of the as-spun alloys are all obtained when Nd content is x = 10. The melt spinning plays a quite beneficial role in the electrochemical discharge capacity and cycle stability of the alloys, and it affects Nd-added alloys more significantly than Nd-free alloy on the electrochemical performances.**

Keywords-Mg_2Ni-type alloy; elemental substitution; melt spinning; nanocrystalline and amorphous; electrochemical characteristics

I. INTRODUCTION

Mg_2Ni-type metallic hydrides are looked upon as one of the most promising hydrogen storage materials applied in hydrogen fuel cell vehicle or negative electrodes in Ni-MH batteries because of their major advantages, such as the higher gaseous hydrogen absorption capacity (3.6 wt%) for Mg_2NiH_4 and the larger theoretical electrochemical capacity (about 1000 mAh/g) [1, 2]. However, the practical application of the alloys is seriously retarded by their relatively high H-desorption temperatures, sluggish hydriding/dehydriding kinetics and very poor electrochemical cycle stability either as the hydrogen storage materials of on-board use or as the negative electrode materials of Ni-MH battery.

It has been ascertained that Mg and Mg-based alloys with a nanocrystalline/amorphous structure exhibit higher hydrogen-absorption capacity and faster hydriding/ dehydriding kinetics than crystalline Mg_2Ni [3]. Melt-spun technique can retard the rapid degradation of hydrogen absorbing/desorbing cyclic characteristics of Mg and Mg-based compounds. In fact, Huang *et al.* [4] reported that the amorphous and nanocrystalline $(Mg_{60}Ni_{25})_{90}Nd_{10}$ alloy prepared by melt-spinning yielded the highest discharge capacity of 580 mAh/g.

Our previous work has confirmed that the substitution of M (M=Cu, Co, Mn) for Ni or La for Mg dramatically improved the gaseous and electrochemical hydrogen storage performances of the Mg_2Ni-type alloys [5]. Therefore, it is expected that the joint addition of Cu and Nd combining a proper melt spinning technique may significantly ameliorate the hydrogen storage characteristics of the Mg_2Ni-type alloy. To validate this, a systematical investigation about the effects of adding Nd and Cu on the structures and electrochemical hydrogen storage performances of as-cast and spun $(Mg_{24}Ni_{10}Cu_2)_{100-x}Nd_x$ (x = 0–20) electrode alloys has been performed.

II. EXPERIMENTAL

The compositions of the experimental alloys were $(Mg_{24}Ni_{10}Cu_2)_{100-x}Nd_x$ (x = 0, 5, 10, 15, 20). For convenience, the alloys were denoted with Nd content as Nd_0, Nd_5, Nd_{10}, Nd_{15} and Nd_{20}, respectively. The alloy ingots were prepared by using a vacuum induction furnace in a helium atmosphere at a pressure of 0.04 MPa to prevent Mg from volatilizing. A part of the as-cast alloys were re-melted and spun by melt spinning with a rotating copper roller cooled by water. The spinning rates used in the experiment were 10, 20, 30 and 40 m/s , which were approximately expressed by the linear velocity of the copper roller.

The phase structures of the as-cast and spun alloys were determined by XRD (D/max/2400). The diffraction, with the experimental parameters of 160 mA, 40 kV and 10°/min respectively, was performed with CuK_α radiation. The thin film samples of the as-spun alloys prepared by using ion etching technology were observed by TEM (JEM-2100F, operated at 200 kV) and their crystalline states were ascertained by electron diffraction (ED).

Mechanical milling was used to pulverize the alloys into fine powder with a diameter of 20μm. Mix the alloy power with carbonyl nickel powder in a weight ratio of 1:4. The mixture was cold pressed under a pressure of 35 MPa into

round electrode pellets with 15 mm in diameter and its total weight is 1 g. The electrochemical measurements were performed at 30 °C by using a tri-electrode open cell consisting of a working electrode (the metal hydride electrode), a sintered $Ni(OH)_2$/NiOOH counter electrode as well as a Hg/HgO reference electrode, which were immersed in 6 M KOH electrolyte. The voltage between the negative electrode and the reference one was defined as the discharge voltage. In every cycle, the alloy electrode was first charged with a constant current density, after resting for 15 min, it was discharged at the same current density to cut-off voltage of –0.500 V.

III. Results and Discussion

A. *Microstructure characteristics*

Shown in Figure 1 are the XRD profiles of the as-cast and the spun (20 m/s) $(Mg_{24}Ni_{10}Cu_2)_{100-x}Nd_x$ (x = 0–20) alloys, indicating that the addition of Nd engenders an evident change in the phase compositions of the as-cast alloys. Obviously, all the as-cast alloys hold multiphase structures. The addition of Nd generates secondary phase $NdMg_{12}$ along with the main phase Mg_2Ni, whose amounts

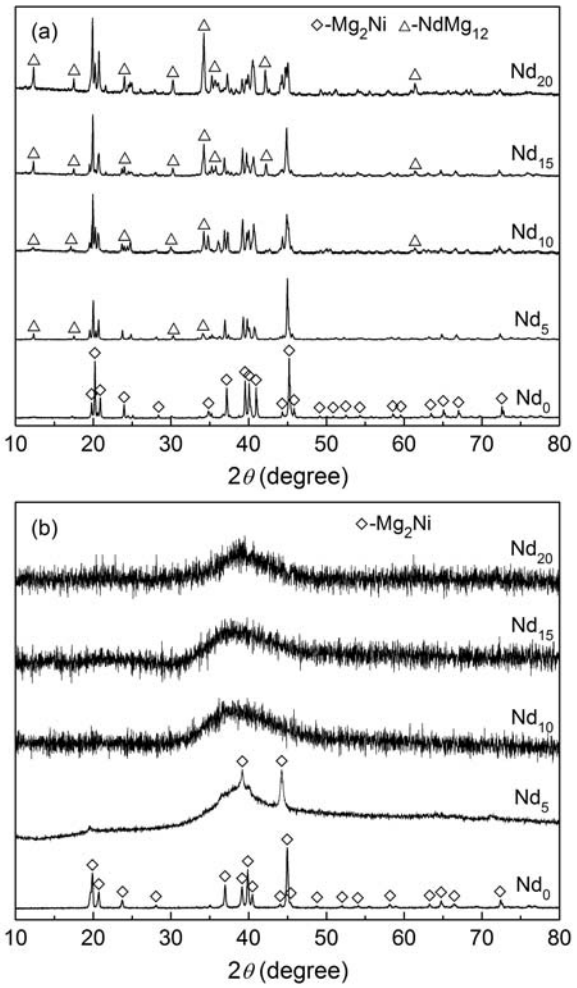

Figure 1. XRD profiles of the as-cast and spun $(Mg_{24}Ni_{10}Cu_2)_{100-x}Nd_x$ (x = 0–20) alloys: (a) as-cast, (b) as-spun (20 m/s).

increase markedly with Nd content rising. Furthermore, it is found that the very sharp diffraction peaks appear in the as-spun Nd_0 alloy, suggesting that it holds an entire crystalline structure. Interestingly, the diffraction peaks of the as-spun alloys are sharply broadened with Nd content increasing, exhibiting an evident nanocrystalline and amorphous mixed structure, implying that the addition of Nd facilitates the glass formation in the Mg_2Ni-type alloy.

The TEM micrographs of the as-spun (20 m/s) $(Mg_{24}Ni_{10}Cu_2)_{100-x}Nd_x$ (x = 0–20) are demonstrated in Figure 2. In order to clearly identify the microstructures of the alloys, the locally amplified morphologies of the as-spun alloys are also presented in Figure 2. It is very evident that the as-spun Nd_0 alloy exhibits an entire nanocrystalline structure, and sharp multi-haloes appears on its electron diffraction (ED) pattern, which corresponds to a crystalline structure. Some crystal defects such as subgrains and grain boundaries can be seen clearly. Differing from Nd_0 alloy, the as-spun Nd_{10} and Nd_{20} alloys exhibit a clear feature of the nanocrystalline embedded in the amorphous matrix, and its electron diffraction pattern consists of broad and dull halo, confirming the presence of an amorphous structure. It is quite evident that the amorphization degree of the as-spun alloys visibly increases with the growing of the amount of Nd addition, which conforms to the XRD observations depicted in Figure 1.

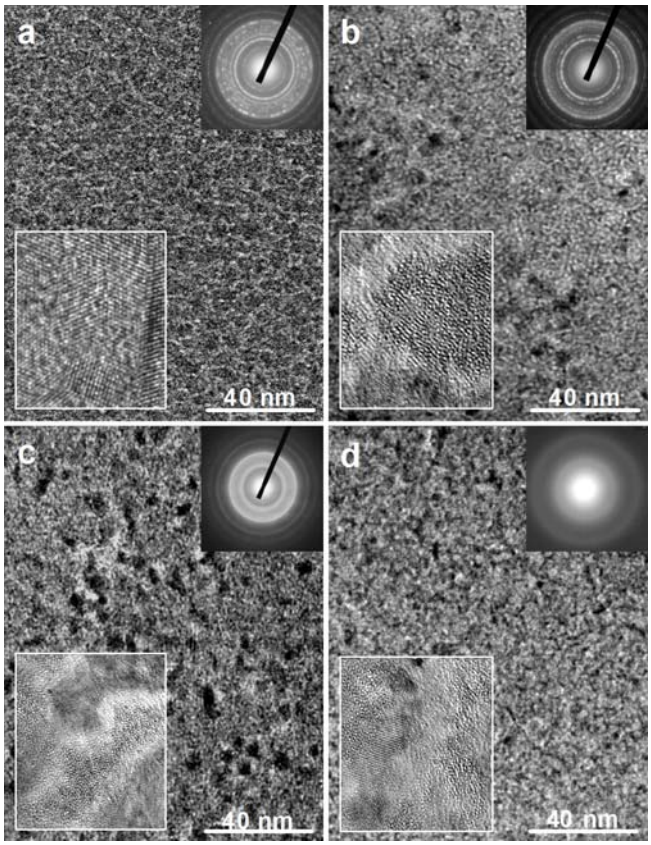

Figure 2. TEM micrographs and ED patterns of the as-spun (20 m/s) $(Mg_{24}Ni_{10}Cu_2)_{100-x}Nd_x$ (x = 0–20) alloys: (a) Nd_0 alloy, (b) Nd_5 alloy, (c) Nd_{10} alloy, (d) Nd_{20} alloy.

B. Electrochemical hydrogen storage characteristics

The variations of the discharge capacity of the as-cast and spun $(Mg_{24}Ni_{10}Cu_2)_{100-x}Nd_x$ (x = 0–20) alloys with cycle number are provided in Figure 3, from which it is found that the as-cast and spun alloys possess superior activation capability, obtaining their maximum discharge capacity at most three charge/discharge cycles. Moreover, it is very evident that whatever the cycle number is, the Nd-added alloys always have higher discharge capacities than that of the Nd-free alloy, suggesting that such addition facilitates the discharge capacity of the alloy upgrading. For the as-cast alloys, the superior activation performance is considered to be related to multiphase structure due to the phase boundary providing good tunnels for hydrogen atoms to diffuse, further improving the activation capability. And with regard to the as-spun alloys, it is ascribed to the nanocrystalline/amorphous structure created by melt spinning because the numerous grain boundaries probably act as buffer areas which can greatly release the lattice distortion and strain energy accumulated during hydrogen absorption process.

The variations of the discharge capacity of the as-cast and spun $(Mg_{24}Ni_{10}Cu_2)_{100-x}Nd_x$ (x = 0–20) alloys with the amount of Nd addition is presented in Figure 4, from which it is found that both the as-cast and spun alloys yield the maximum discharge capacity when Nd content is x = 10. It

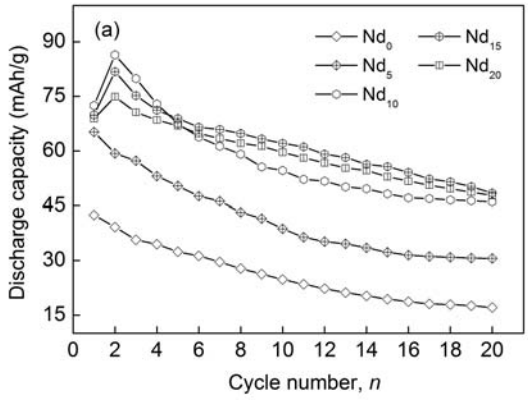

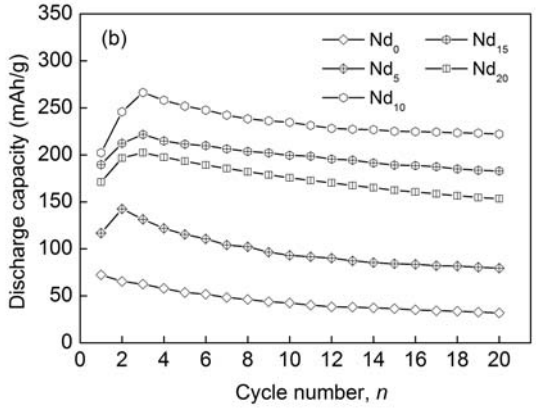

Figure 3. Activation capability of the as-cast and spun the $(Mg_{24}Ni_{10}Cu_2)_{100-x}Nd_x$ (x = 0–20) alloys: (a) as-cast, (b) as-spun (20 m/s).

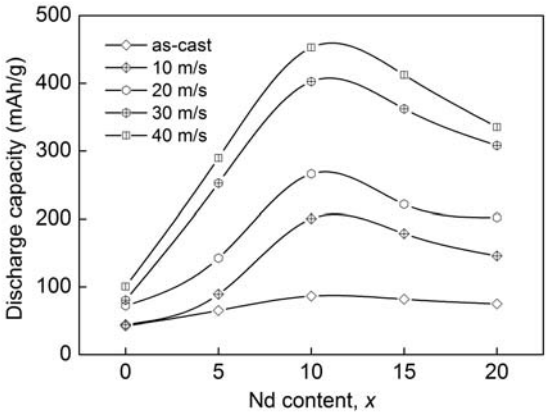

Figure 4. Evolution of the discharge capacity of the as-cast and spun the $(Mg_{24}Ni_{10}Cu_2)_{100-x}Nd_x$ (x = 0–20) alloys with Nd content.

must be mentioned that, whatever the spinning rate is, the Nd-added alloys show a visibly higher discharge capacity than the Nd-free one, indicating that the addition of Nd brings on a positive impact on the discharge capacity of Mg_2Ni alloy. In addition, we note that, for the fixed Nd content, the discharge capacity of the alloy significantly upgrades with the spinning rate increasing. Particularly, when the spinning rate grows from 0 to 40 m/s (the as-cast is defined as the spinning rate of 0 m/s), the discharge capacity is enhanced from 42.5 to 100.6 mAh/g for the Nd_0 alloy and from 86.4 to 402.5 mAh/g for the Nd_{10} alloy, respectively. Evidently, melt spinning engenders a more distinguished improvement on the discharge capacity of the Nd-added alloys compared to the Nd-free one. The facilitated glass forming ability originated from adding Nd is beneficial to the discharge capacity of the alloy because an adequate proportion of amorphous and nanocrystalline in Mg-Ni-based alloy possesses superior discharge property [6]. The excessive amount of Nd (x > 10) gives rise to an undesired reduction in the discharge capacity, for which the sharp decrease of the Mg_2Ni phase is mainly responsible. With regards to the improvement of discharge capacity introduced by melt spinning, it is definitely associated with

nanocrystalline and amorphous structure owing to the grain boundaries possessing the distribution of the maximum hydrogen concentrations. Also, the nanocrystalline and amorphous structure generated by melt spinning evidently promotes the hydriding and dehydriding abilities of Mg_2Ni-type alloys [7].

Cycle stability, one of the major criteria for practical applicability of Ni/metal hydride systems for reversible hydrogen storage, is signified by the capacity retaining rate (S_n), defined as $S_n = C_n/C_{max}\times100$ (%), where C_{max} is the maximum discharge capacity and C_n is the discharge capacity at the n^{th} charge-discharge cycle, respectively. Apparently, the larger the S_n is, the better the cycle stability of the alloy will be. The S_{20} (n = 20) values of the $(Mg_{24}Ni_{10}Cu_2)_{100-x}Nd_x$ (x = 0–20) alloys with Nd content are described in Figure 5. Interestingly, adding Nd brings on a very different impact on the cycle stability of the as-cast and

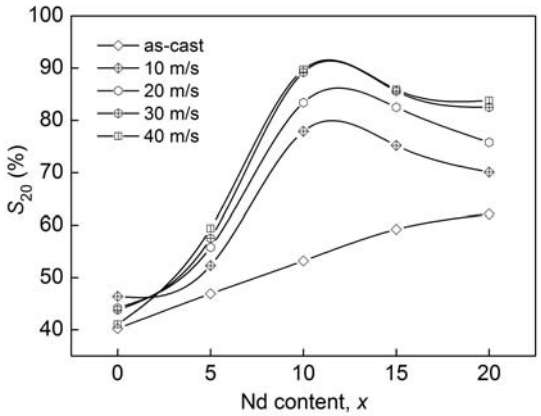

Figure 5. Evolution of the S_{20} values of the as-cast and spun the $(Mg_{24}Ni_{10}Cu_2)_{100-x}Nd_x$ (x = 0–20) alloys with Nd content.

spun alloys. It is clear that the S_{20} values always augment with the growing of Nd content for the as-cast alloy, whereas the maximum values appear for the as-spun ones with Nd content varying. We also find from Figure 5 that, no matter what the state of the alloy is, the Nd-added alloys have much higher S_{20} value than the Nd-free one, indicating that the addition of Nd is beneficial to the improvement of the cycle stability of the Mg_2Ni-type alloy.

It has been ascertained that the rapid degradation of the discharge capacity of Mg_2Ni phase during the charge-discharge cycling results from the formation and thickening of $Mg(OH)_2$ surface layer which hinders the hydrogen atoms from diffusing in or out of the alloy bulk in alkaline solutions [8]. Moreover, the hydrogen storage material suffers a volume change during the charge-discharge process, which aggravates the alloy's cracking and pulverizing and then makes the surface of the material apt to be oxidized. Also, the metastable structures formed by melt spinning or ball milling tends to vanish during multiple charge-discharge cycles, which is an important factor for the capacity decay of the alloy. Generally, the beneficial effect of Nd addition on the cycle stability of the alloy is ascribed to the following several aspects. Firstly, the glass formation facilitated by adding Nd is extremely important because an amorphous phase improves not only anti-pulverization ability but also anti-corrosion and anti-oxidation abilities of the alloy electrode in a corrosive electrolyte [5]. Secondly, the enlarged cell volume caused by adding Nd decreases the ratios of expansion/contraction in the process of hydrogen absorption/desorption, thus increasing the anti-pulverization capability. What is more, the addition of a third element significantly stabilizes the nanostructure of the as-spun alloy [4], which also makes its cycle stability enhanced.

IV. Conclusions

The major phase of the as-cast alloy is Mg_2Ni, the addition of Nd brings on the generation of the $NdMg_{12}$ phases. The addition of Nd facilitates to enhance the glass forming ability of the Mg_2Ni-type alloy and the amorphization degree of the alloys visibly increases with Nd content growing. The addition of Nd gives rise to an augment in the electrochemical discharge capacity and cycle stability of the as-cast and spun alloys, and the maximum discharge capacities and the capacity retaining rate of the as-spun alloys are all obtained when Nd content is x = 10. The melt spinning plays a quite beneficial role in the electrochemical discharge capacity and cycle stability of the alloys, and it affects Nd-added alloys more significantly than Nd-free alloy on the electrochemical performances.

Acknowledgment

This work was financially supported by the National Natural Science Foundations of China (51161015 and 51371094).

References

[1] A. Ebrahimi-Purkani, and S. F. Kashani-Bozorg, "Nanocrystalline Mg_2Ni-based powders produced by high-energy ball milling and subsequent annealing," J. Alloys Compd. vol. 456, pp. 211–215, 2008.

[2] L. Schlapbach, and A. Züttel, "Hydrogen-storage materials for mobile applications," Nature vol. 414, pp. 353–358, 2001.

[3] E. A. Lass, "Hydrogen storage measurements in novel Mg-based nanostructured alloys produced via rapid solidification and devitrification," Int. J. Hydrogen Energy vol. 36, pp. 10787–10796, 2011.

[4] L. J. Huang, G. Y. Liang, Z. B. Sun, and D. C. Wu, "Electrode properties of melt-spun Mg-Ni-Nd amorphous alloys," J. Power Sources vol. 160, pp. 684–687, 2006.

[5] Y. H. Zhang, C. Zhao, T. Yang, H. W. Shang, C. Xu, and D. L. Zhao, "Comparative study of electrochemical performances of the as-melt $Mg_{20}Ni_{10-x}M_x$ (M = None, Cu, Co, Mn; x = 0, 4) alloys applied to Ni/metal hydride (MH) battery," J. Alloys Compd. vol. 555, pp. 131–137, 2013.

[6] T. Spassov, and U. Köster, "Hydrogenation of amorphous and nanocrystalline Mg-based alloys," J. Alloys Compd. vol. 287, pp. 243–250, 1999.

[7] L. H. Kumar, B. Viswanathan, and S. S. Murthy, "Hydrogen absorption by Mg_2Ni prepared by polyol reduction," J. Alloys Compd. vol. 461, pp. 72–76, 2008.

[8] X. Y. Zhao, Y. Ding, L. Q. Ma, L. Y. Wang, M. Yang, and X. D. Shen, "Electrochemical properties of $MmNi_{3.8}Co_{0.75}Mn_{0.4}Al_{0.2}$

hydrogen storage alloy modified with nanocrystalline nickel," Int. J. Hydrogen Energy vol. 33, pp. 6727–6733, 2008.